Improved Microwave Radiometric Imaging of Surface Wind Speed Dynamics in the Hurricane Eye-Wall

Ruba Amarin, W. Linwood Jones
Central Florida Remote Sensing Lab.
The University of Central Florida
Orlando, Florida
*ramarin@mail.ucf.edu

Christopher Ruf
Space Physics Research Laboratory
University of Michigan
Ann Arbor, Michigan

Shuyi Chen
University of Miami
Miami, Florida

ABSTRACT

This paper addresses one critical aspect of the HIRAD design, namely, the antenna spatial sampling and its impact on the information content of the retrieved ocean surface wind field. Specifically, this paper presents simulated results of HIRAD measurements of the wind field in the region of a hurricane eye-wall, and of the curl of the wind derived from the measurements. High resolution numerical model wind fields from Frances 2004 are convolved with various HIRAD antenna spatial filters to observe the impact of the antenna design on the curl, and on the central pressure depression in the eye that can be deduced from it.

1. INTRODUCTION

The Hurricane Imaging Radiometer, HIRAD, a next-generation airborne microwave remote sensor under development by NASA, will expand the airborne hurricane measurement capabilities of two existing state-of-the-art microwave radiometers; the Stepped Frequency Microwave Radiometer, SFMR, and the Lightweight Rainfall Radiometer, LRR. HIRAD combines the multi-freqiency C-band channels of SFMR with the “push-broom” surface imaging of the LRR Synthetic Thinned Array Radiometrey (STAR) to provide improved footprint resolution of (~2 km), over a wide-swath that reaches to (~ 3 x AC altitude). HIRAD provides images of the ocean surface wind speed and near-surface rain rate in a hurricane environment. Because of its wide-swath imaging, HIRAD can significantly improve the detection of peak winds in hurricanes. This will result in more accurate hurricane intensity classification and better numerical model forecast prior to landfall.

2. DESCRIPTION OF THE ORIGINAL DATA SET (THE MODELED HURRICANE WIND FIELD)

Hurricane Frances’ wind field was used as the model from which the observations are simulated. The simulations were used from the state-of-art system described by Chen et al. (2007). The simulations use a system of nested grids with the innermost one having a horizontal grid spacing of 0.015 degrees (~1.6 km) in longitude and latitude. The model is non-hydrostatic in the atmosphere with detailed explicit microphysics and an interactive ocean wave model. The results include an eyewall, rainbands and other realistic convective and mesoscale structure.

The HIRAD sampling, as currently implemented, constructs cross-track scans with each gridded wind speed value so that the spatial resolution over the HIRAD field-of-view is of the same size as the model grid both cross-track and along track. Contiguous scans are formed along the track in a pushbroom fashion as the platform flies along. For the wind field shown in Fig. 1, the swath for a typical HIRAD pass through the eye with the aircraft at 20 km would extend to cover the full eye-wall region.

The wind field shown in Fig. 1 has a maximum value of 55 m/s in the eye wall region. A north-to-south transect, with the ground track indicated in pink, was used in these analysis for hurricane Frances, HR 24 on August 31st , 2004, as shown in Fig. 1.

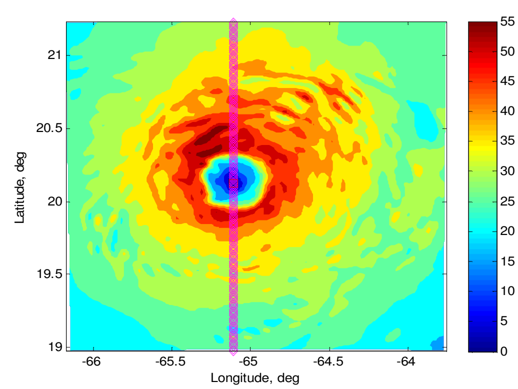

Figure 1 Hurricane Frances wind field (m/s) at HR 24 on 31 August, 2004. Wind speed is represented by the color scale for an A/C flying from north-to-south through the hurricane eye

3. PRESSURE DEPRESSION ESTIMATION (PDE) ALGORITHM

The magnitude of the curl of the wind field was computed for the north-to-south transect through the eye of hurricane Frances.

Two regions were defined in a simplified hurricane model; a rotational and an irrotational flow region. A relationship between velocity and radial distance for both regions was developed. Assuming that the eye wall region is rotational, the curl of the flow velocity is given by

$$curl\, v = 2\omega \tag{1}$$

Where ω is the angular velocity in rad/sec. As a function of radial distance, *r*, from the center, ω is given by

$$\omega = \frac{v}{r} \tag{2}$$

A typical max value for the curl computed from the wind field for the Frances data is 5.8×10^{-3} rad/sec. This is consisent with the peak wind velocity of 65.8 m/s at a radial distance of 22.7 km.

To calculate the pressure, *P*, the centripatal acceleration can be related to the pressure gradient force according to Kleinstreuer (1997)

$$\rho \frac{v^2}{r} = \frac{dp}{dr} \tag{3}$$

where the pressure force refers to the horizontal movement of air according to

$$\rho \frac{F}{m} = -grad\ P \tag{4}$$

The term F/m in (4) is equal to the acceleration, dv/dt, according to Newton's law $F = ma$. The pressure gradient has three components; dp/dx, dp/dy and dp/dz along the x, y and z-axes, respectively. ρ is the mass density, which increases with acceleration as the presure decreases. The pressure gradient force acts at right angles to isobars in the direction from high to low pressure. The greater the pressure difference over a given horizontal distance, the greater the force and, hence, the stronger the wind.

The differential equation in (3) can be integrated for the two different regions, producing an expression for the pressure in the irrotational region given by

$$\begin{aligned} P &= P_\infty - \rho \frac{v^2}{2} \\ &= P_\infty - \rho \frac{(\omega r)^2}{2} \end{aligned} \tag{5}$$

where, P_∞ is the pressure outside of the cyclonic region for hurricane Frances, HR 24, where a maximum pressure of 1012.7 mbar was reported in the modeled data. The density value was tuned by substituting P_∞ in (5), using the model value for minimum pressure in the eye (934.44 mbar), and computing the estimated density of **ρ** = 3.56 kg/m^3.

4. RESULTS

A variety of spatial running average filters were applied to the original wind field model shown in Fig. 1. A square filter with different window sizes of 3x3, 5x5, 7x7 and 9x9 was applied to the U and V components of the wind speed, producing a new, filtered, wind field. This is a "box-car" simulation of the HIRAD antenna pattern with variable beamwidth. The original, unfiltered wind field data is modeled at 1.67 km spatial resolution, which, for example, makes the 3x3 filtered resolution 3 times that. The curl was then computed for the filtered wind field to estimate the 'rate of rotation', given as the magnitude of the curl. Its magnitude describes how much rotation there is and the vector direction indicates which axis the field is rotating about. Figure 2 shows line plots of the z-component of the curl, which is equal to twice the angular velocity, for a 3x3 and 9x9 window size along with the unfiltered curl for comparison.

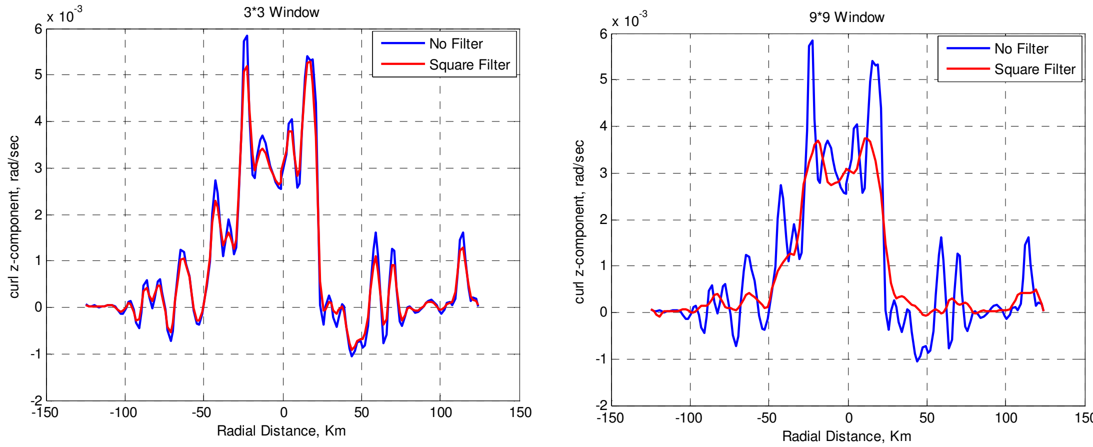

Figure 2 The z-component of curl for a 3x3 and a 9x9 square spatial filter window along with the unfiltered curl (blue)

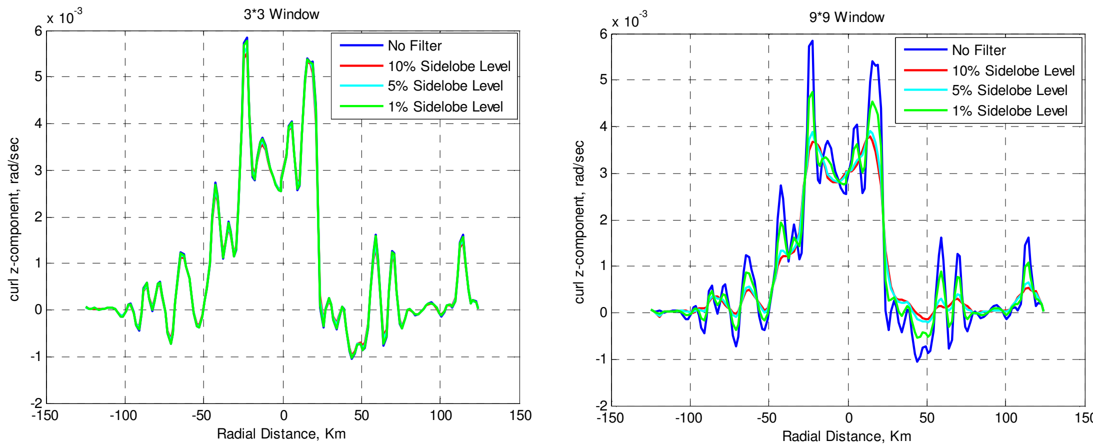

Figure 3 The z-component of curl for a 3x3 and a 9x9 top hat on a pedestal filter window along with the unfiltered curl (blue)

The magnitude of the curl decreases as the window filter size increases, which simulates spatial smoothing by increasing size of the antenna footprint. The maximum curl value reported for a 3x3 window was 0.0053 rad/sec while for a 9x9 window the value was 0.0038 rad/sec. These values will be used to compute a pressure estimate inside the eye wall region.

Another idealized spatial filter that was considered is the "top hat". It is a running average window in which the central portion of the window is 1x1 and the rest of the window is a constant and smaller value. This filter was considered to model the antenna sidelobe structure. The value of the sidelobe level was varied to equal 1%, 5% and 10% of the magnitude of the central top hat portion, which represented a variable antenna beam efficiency for the various spatial filter sizes. The point of a simulation like this is to separate apart the impacts of antenna beam width and sidelobe level on the derived wind field products. Figure 3 contains the z-component of the curl for 3x3 and 9x9 window sizes and for three different side lobe levels, along with the unfiltered curl.

For a 3x3 window, results show that there is not a significant difference in the computed curl between the three different sidelobe levels, whereas, for a 9x9 window, the 10% sidelobe level had the maximum effect on the computed curl.

The pressure was then calculated from the maximum curl values for each window size for both filters and the corresponding radial distances. This was done for the transect in Fig. 1 passing through the eye-wall both entering and exiting the eye. Figure 4 shows the error in the pressure depression estimate as a function of spatial resolution on each side of the eye wall, where the

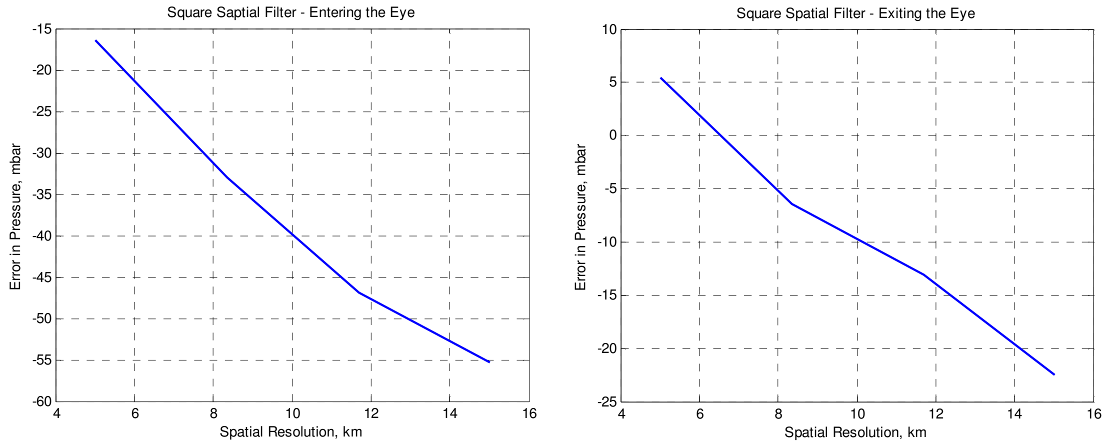

Figure 4 Error in the pressure depression estimate as a function of spatial resolution

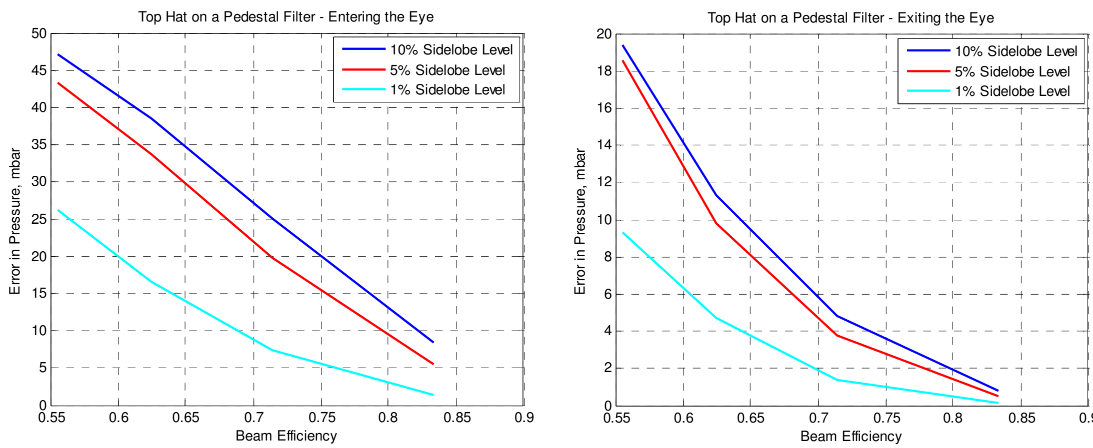

Figure 5 Error in the pressure depression estimation as a function of beam efficiency

3x3, 5x5, 7x7 and 9x9 window sizes correspond to 3x, 5x, 7x and 9x1.67 km resolution, respectively.

Results show a continuous increase in the magnitude of the pressure error as the spatial resolution increases. The dramatic effect on error in estimated pressure for the 9x9 window over the 3x3 is due to the averaging, or smoothing, of the wind field over the larger HIRAD footprint.

Radial distance, or the location of the maximum curl, also changes with spatial resolution, or filter size. Since pressure is a function of both maximum curl and radial distance in (5) this also contributes to the errors in Fig. 4. Results showed a maximum error in estimated radial distance of 3.34 km (2 pixels) for the maximum curl both entering and exiting the eye-wall.

Figure 5 shows the error in the pressure depression estimation as a function of beam efficiency for a “top hat” filter for each side of the eye wall.

Results show that the error in pressure is smaller for the 1% sidelobe level filter and that errors increase with the magnitude of the side lobe level. Again, the error in radial distance was computed as a function of beam efficiency. Results showed a zero difference on the entering side while there is a maximum error of 1.67 km (1 pixel) for the exiting side. Most microwave radiometer antennas would be designed for a beam efficiency of approximately 90 percent, or greater, which would not contribute significant error according to these results. HIRAD offers a trade-off between beam efficiency and swath that might be exploited, but with these results in mind.

The following tables summarize these results.

	Parameters	No Filter	Square Filter			
			3×3	5×5	7×7	9×9
Entering the Eye	Max. Curl (rad/sec)×10^{-3}	2.92	2.59	2.22	1.99	1.85
	Radial Distance (km)	22.7	22.7	22.7	21.0	19.3
	Pressure (mbar)	935	951	968	982	990
Exiting the Eye	Max. Curl (rad/sec)×10^{-3}	2.70	2.64	2.41	2.07	1.88
	Radial Distance (km)	15.7	17.4	15.7	15.7	12.4
	Pressure (mbar)	981	975	987	994	1003

	Parameters	Top Hat Filter											
		1%				5%				10%			
		3×3	5×5	7×7	9×9	3×3	5×5	7×7	9×9	3×3	5×5	7×7	9×9
Entering the Eye	Max. Curl (rad/sec)×10^{-3}	2.89	2.78	2.59	2.38	2.82	2.52	2.20	1.95	2.76	2.41	2.08	1.84
	Radial Distance (km)	22.7	22.7	22.7	22.7	22.7	22.7	22.7	22.7	22.7	22.7	22.7	22.7
	Pressure (mbar)	936	942	951	961	940	954	968	978	943	960	973	982
Exiting the Eye	Max. Curl (rad/sec)×10^{-3}	2.69	2.64	2.49	2.27	2.68	2.54	2.25	1.96	2.66	2.49	2.17	1.9
	Radial Distance (km)	15.7	15.7	15.7	15.7	15.7	15.7	15.7	14.6	15.7	15.7	15.7	14.6
	Pressure (mbar)	981	982	985	990	981	984	990	999	981	985	992	1000

5. SUMMARY

Different HIRAD antenna spatial filters were used to simulate various antenna pattern characteristics. The central pressure depression was computed in the eye wall region of hurricane Frances using maximum curl estimates. Increasing the spatial resolution and decreasing the beam efficiency both cause an underestimation of the maximum curl, generally, and may also affect the radial distance for maximum curl. Therefore, both generally cause minimum pressure to be over estimated. Error in pressure due to low beam efficiency , which is relatively small at approximately 10 mbar or less, was observed for reasonable beam efficiency values of approximately 80% or higher. Errors due to increasing spatial resolution from 1.67 km (which is achievable by HIRAD from aircraft altitudes) to 4 km - 15 km was approximately 10 mbar to greater than 50 mbar for this analysis. These results suggest that spatial resolution of a few km or better are required to estimate minimum pressure in the hurricane eye to better than 10 mbar.

6. REFERENCE

Chen, S. S., J. F. Price, W. Zhao, M. A. Donelan, E. J. Walsh, 2007: The CBLAST-Hurricane Program and the Next-Generation Fully Coupled Atmosphere–Wave–Ocean Models for Hurricane Research and Prediction. Bull. Amer. Meteor. Soc., 88(3), 311-317.

Kleinstreuer, C., 1997: *Derivations and Transformations of the conservation Equations*.